Recent progress in multi-wavelength observations of core-collapse supernovae

Takashi Moriya
National Astronomical Observatory of Japan

国立天文台
NAOJ
National Astronomical Observatory of Japan

Observational properties of core-collapse SNe

- hydrogen-rich SNe (Type II)
- stripped-envelope (no or little hydrogen) SNe (Type IIb, Ib, Ic, Ic-BL)

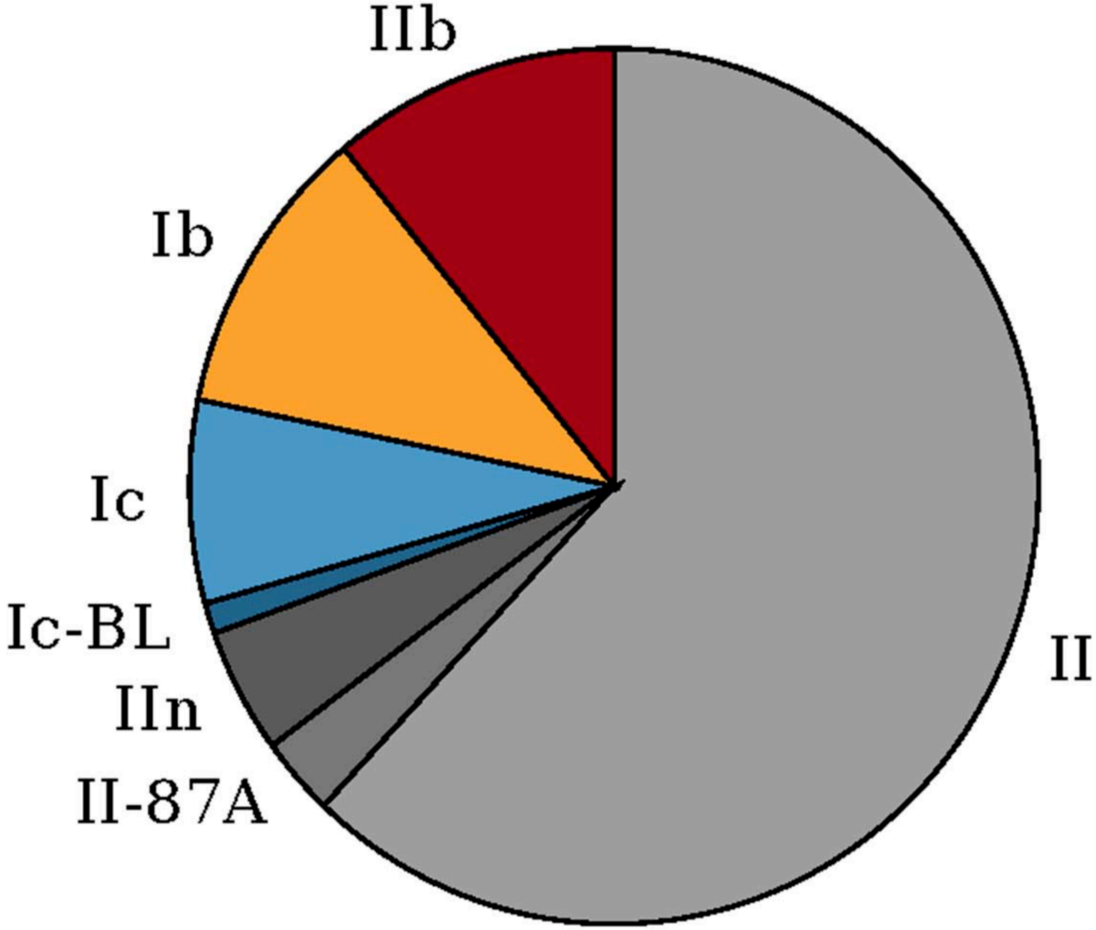

Shivvers et al. (2017)

Standard luminosity source of core-collapse SNe

- thermal energy from the initial shock
  - significant for extended progenitors (mostly H-rich progenitors)

- nuclear decay of ^{56}Ni synthesized during the explosion

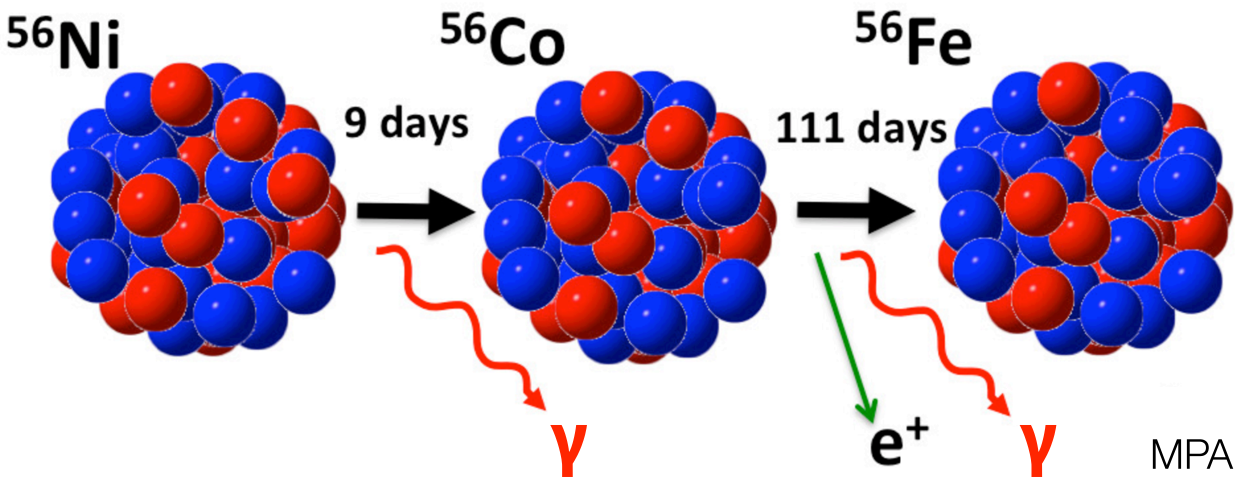

MPA

Hydrogen-rich SNe

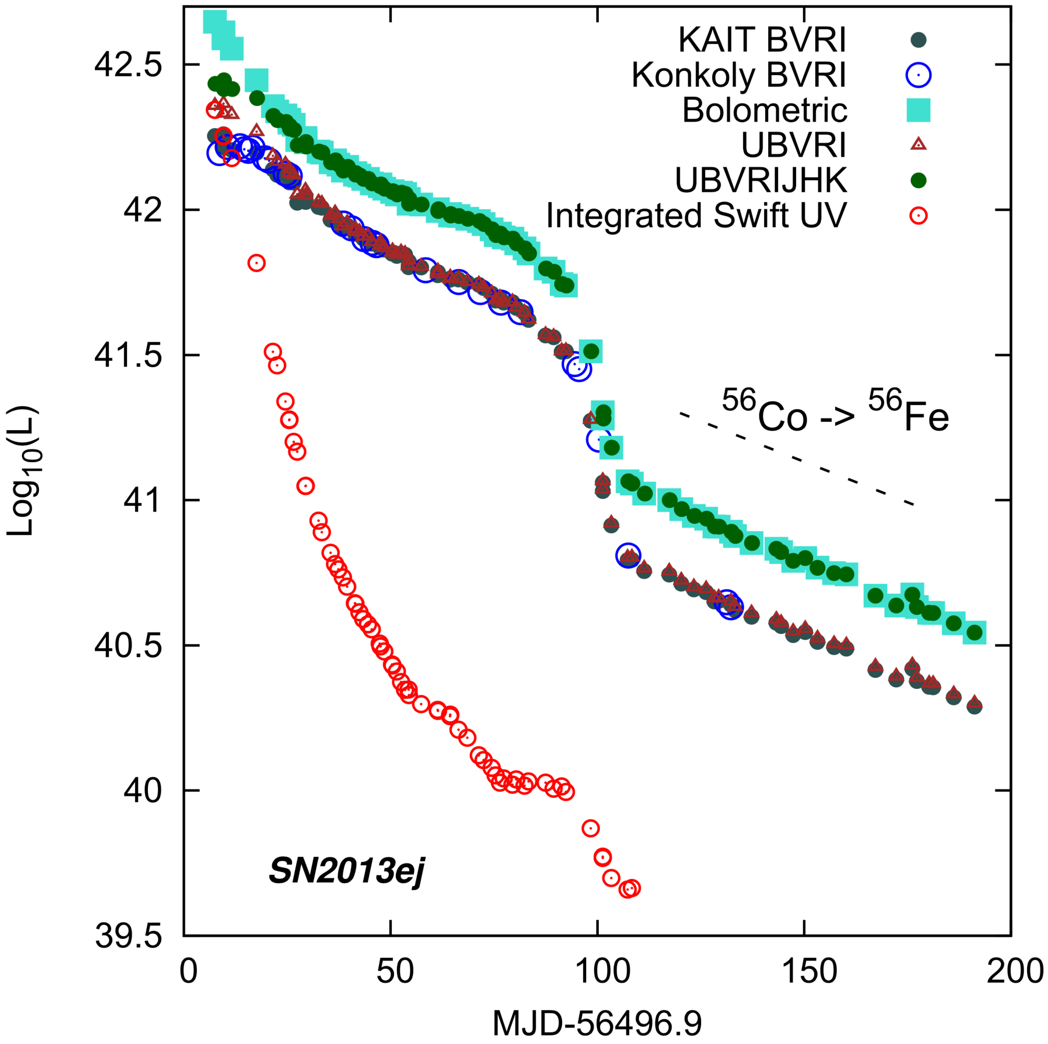

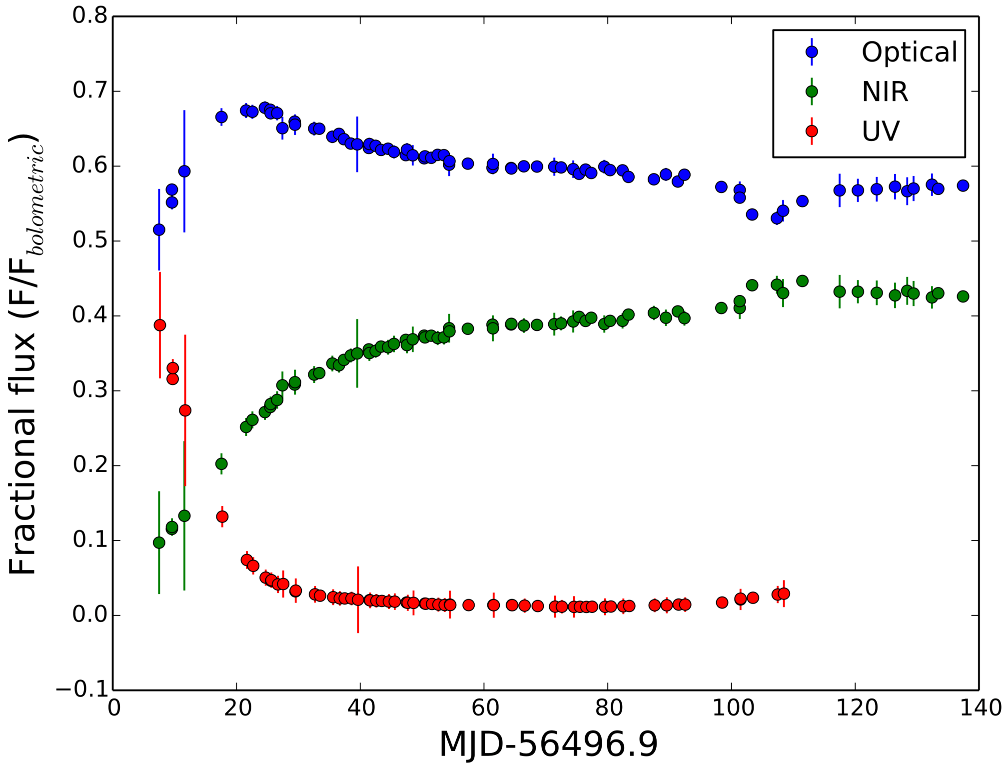

Dhungana et al. (2017)

^{56}Ni mass of hydrogen-rich SNe

SN distribution (N)	Mean ($M_\odot$)	Standard deviation ($M_\odot$)	Median ($M_\odot$)	Max ($M_\odot$)	Min ($M_\odot$)
SN II (115)	0.044	0.044	0.032	0.360	0.001

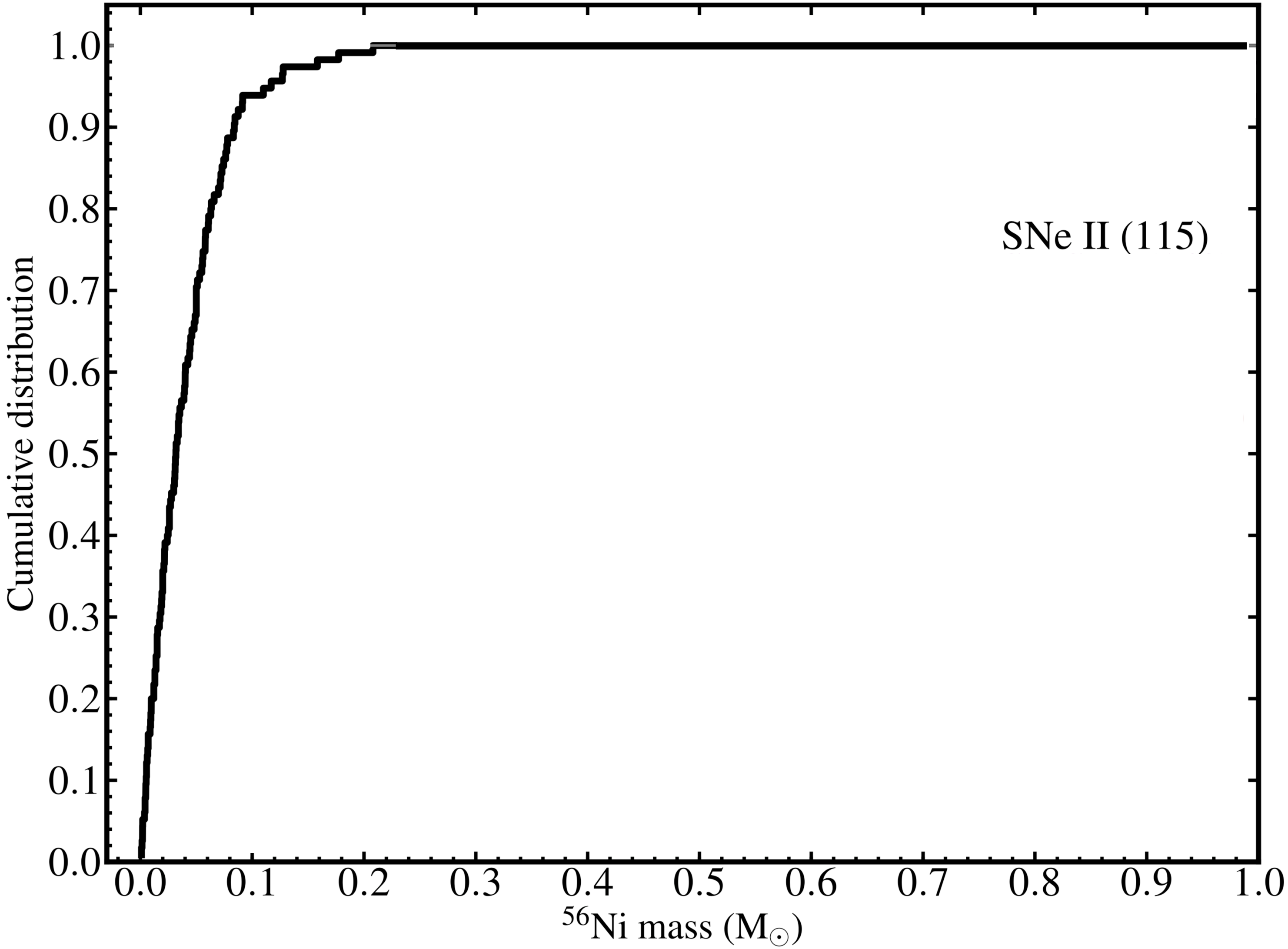

Anderson (2019)

Estimating explosion properties

$$\log(E_{51}) = -0.728 + 2.148\log(L_{42}) - 0.280\log(M_{\rm Ni}) + 2.091\log(t_{\rm p,2}) - 1.632\log(R_{500}),$$

$$\log(M_{10}) = -0.947 + 1.474\log(L_{42}) - 0.518\log(M_{\rm Ni}) + 3.867\log(t_{\rm p,2}) - 1.120\log(R_{500}),$$

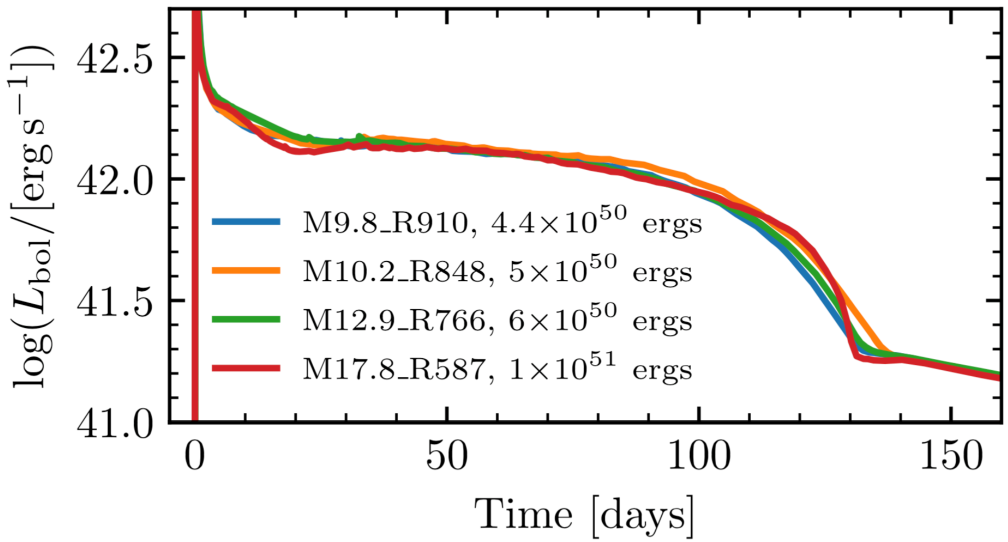

Goldberg et al. (2019)

Velocity evolution

$$\log(v_{\rm Ph,15}) = 3.90 - 0.22\log(M_{10}) + 0.43\log(E_{51}) - 0.13\log(R_{500})$$

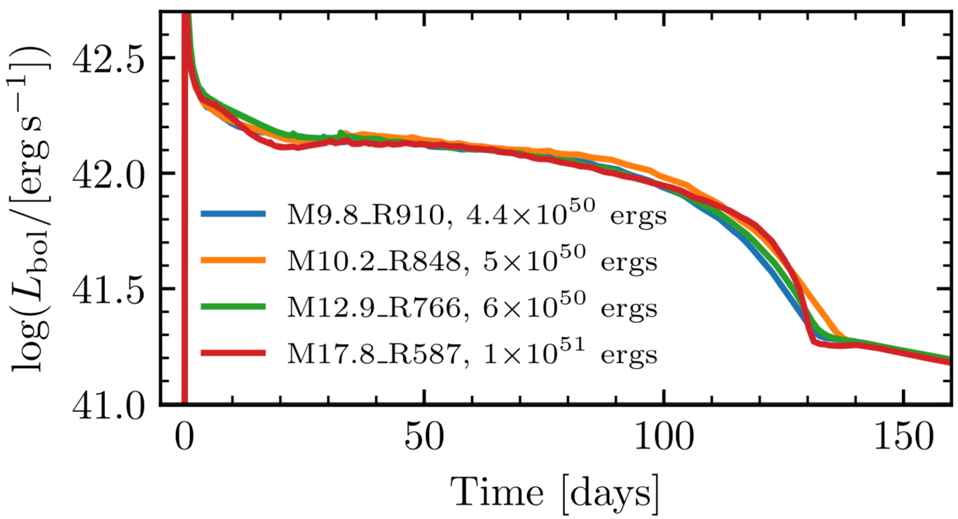

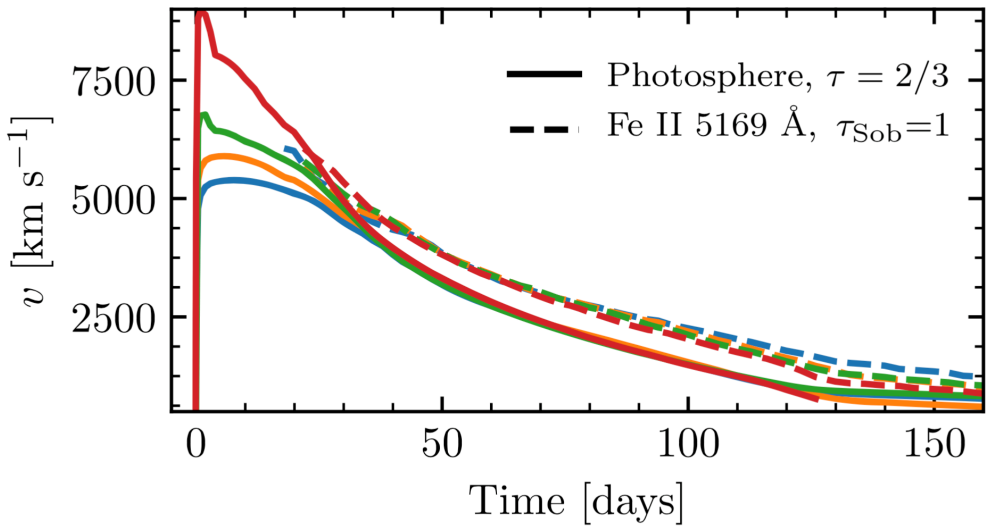

Goldberg et al. (2019)

Early phase affected by circumstellar interaction

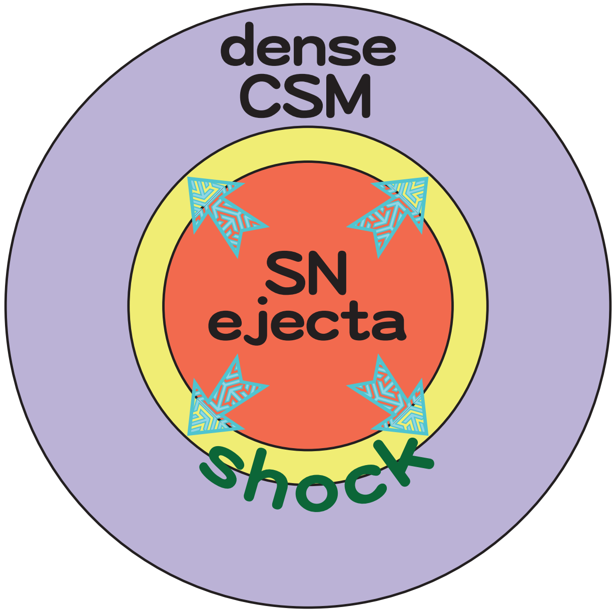

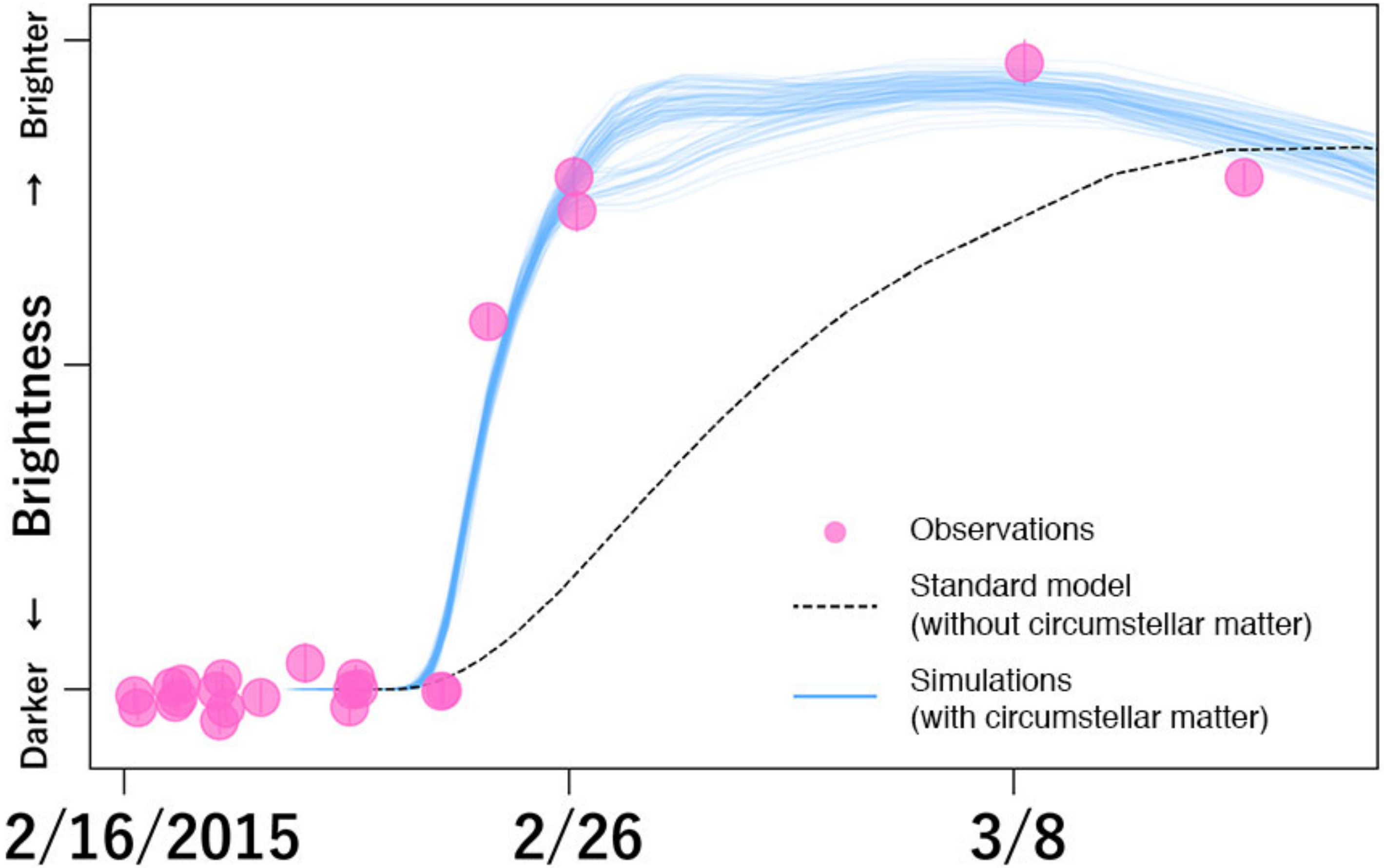

Credit: Förster et al. Nature Astronomy 2018, modified

Förster, Moriya et al. (2018)

Early phase affected by circumstellar interaction

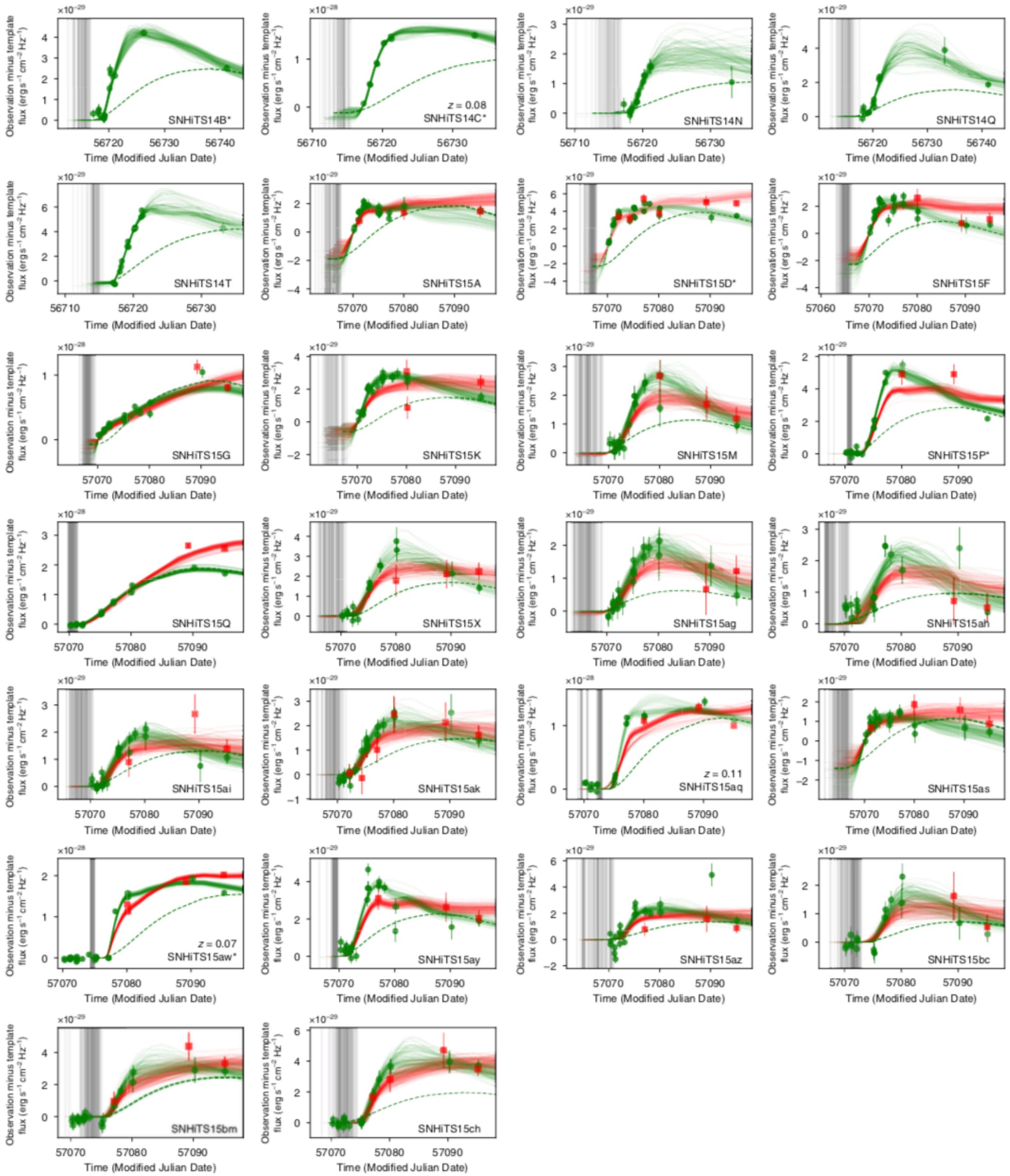

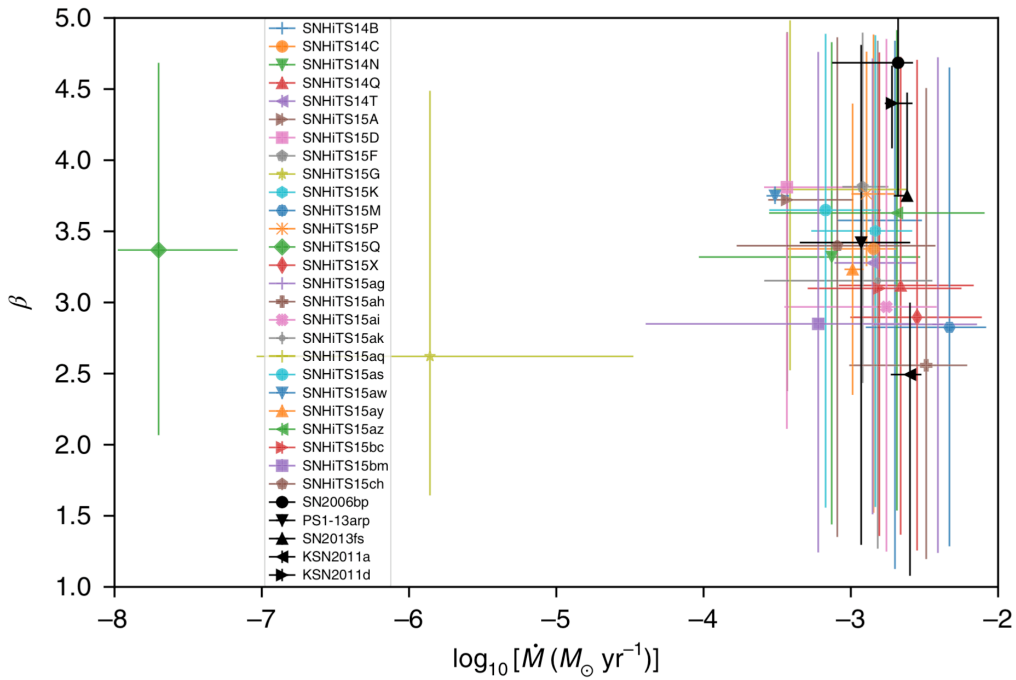

Förster, Moriya et al. (2018)

Velocity evolution with dense CSM

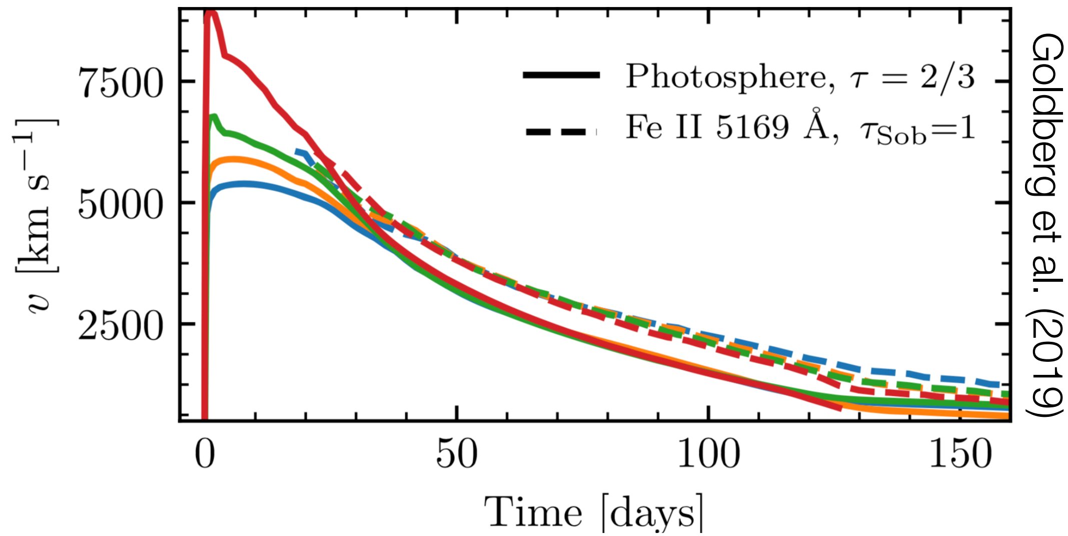

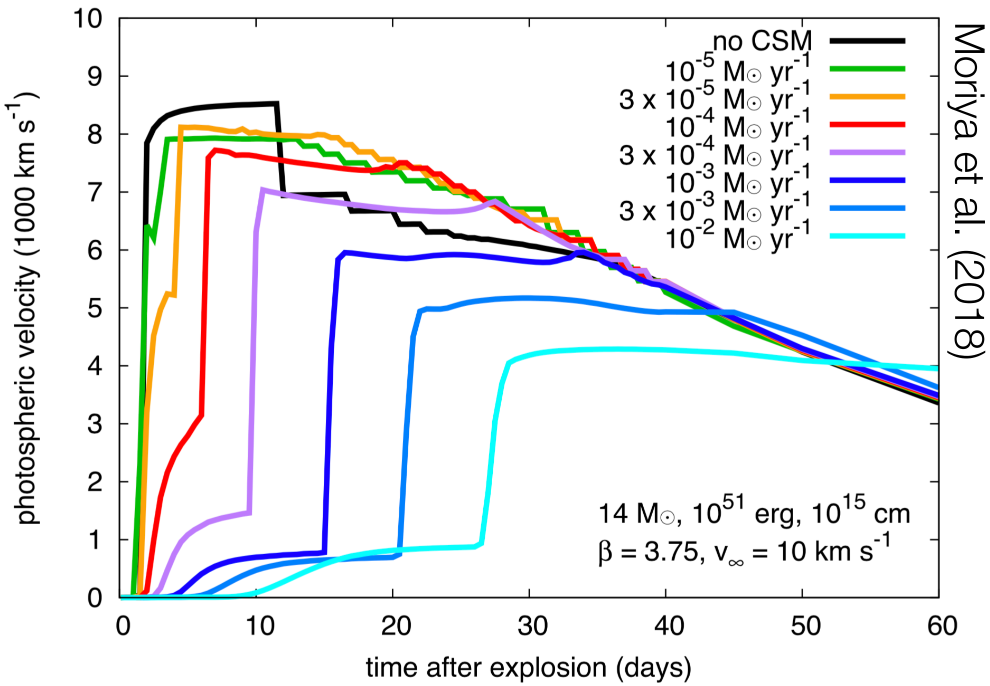

Radius from the progenitor direct imaging

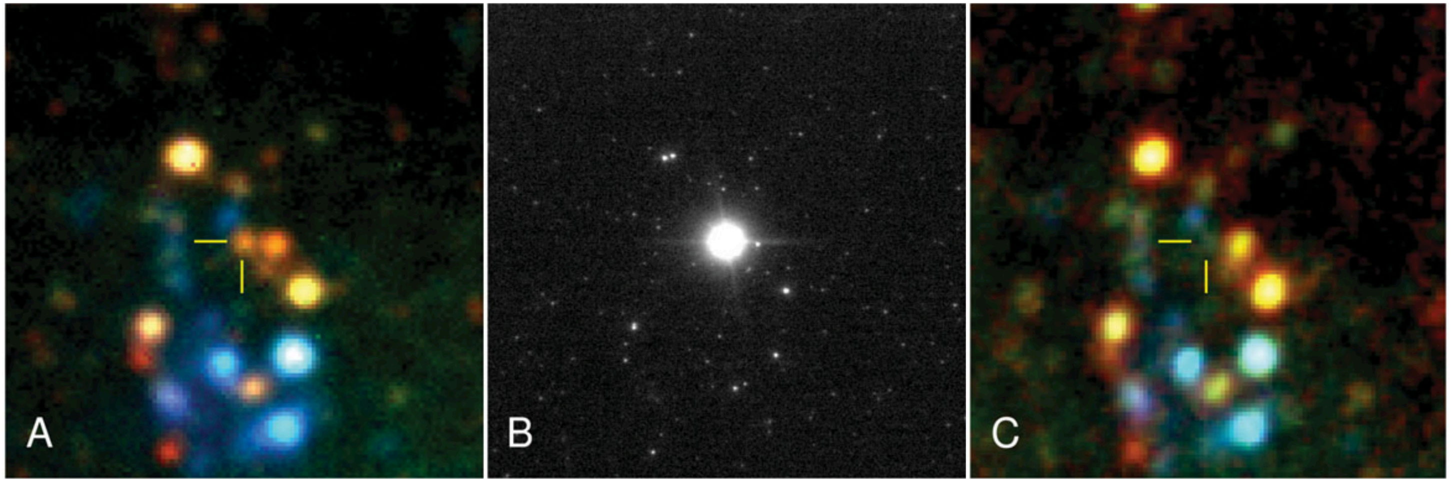

Smartt (2015)

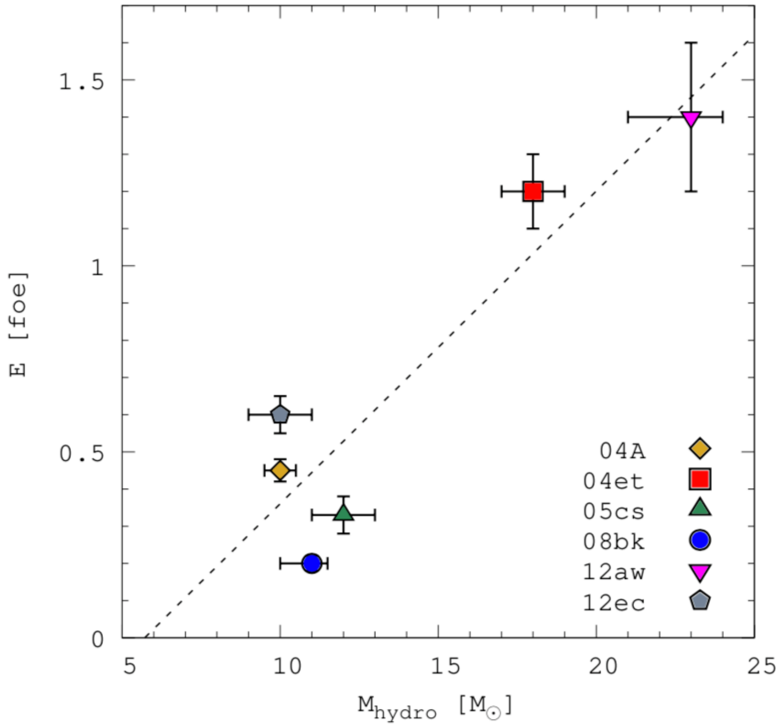

Martinez et al. (2019)

Stripped-envelope SNe

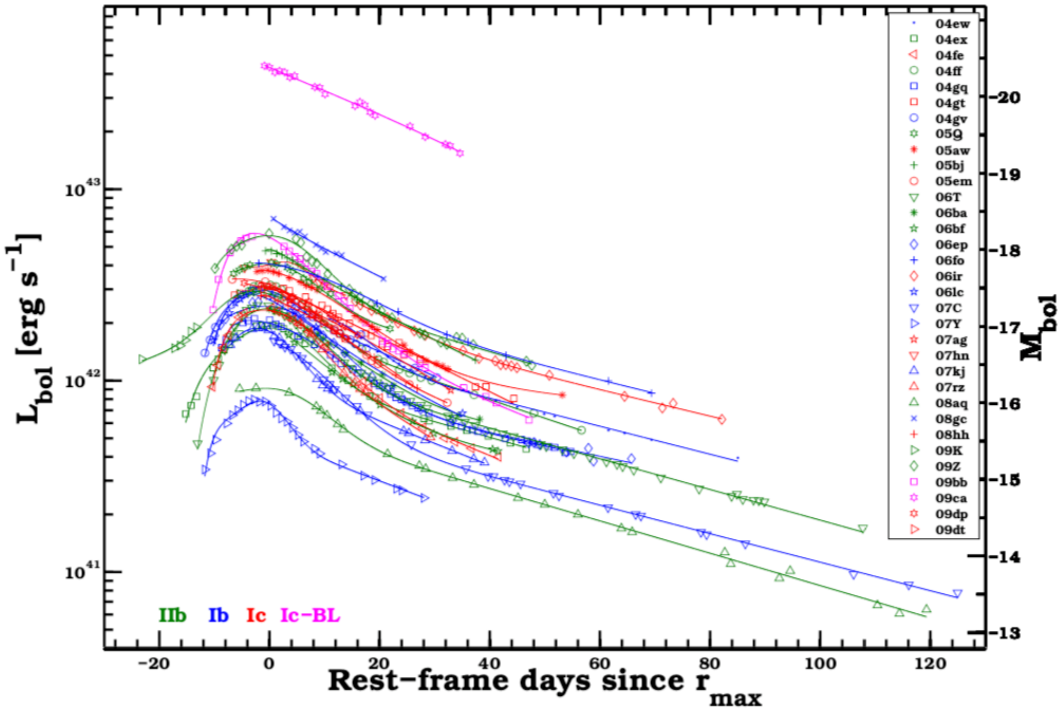

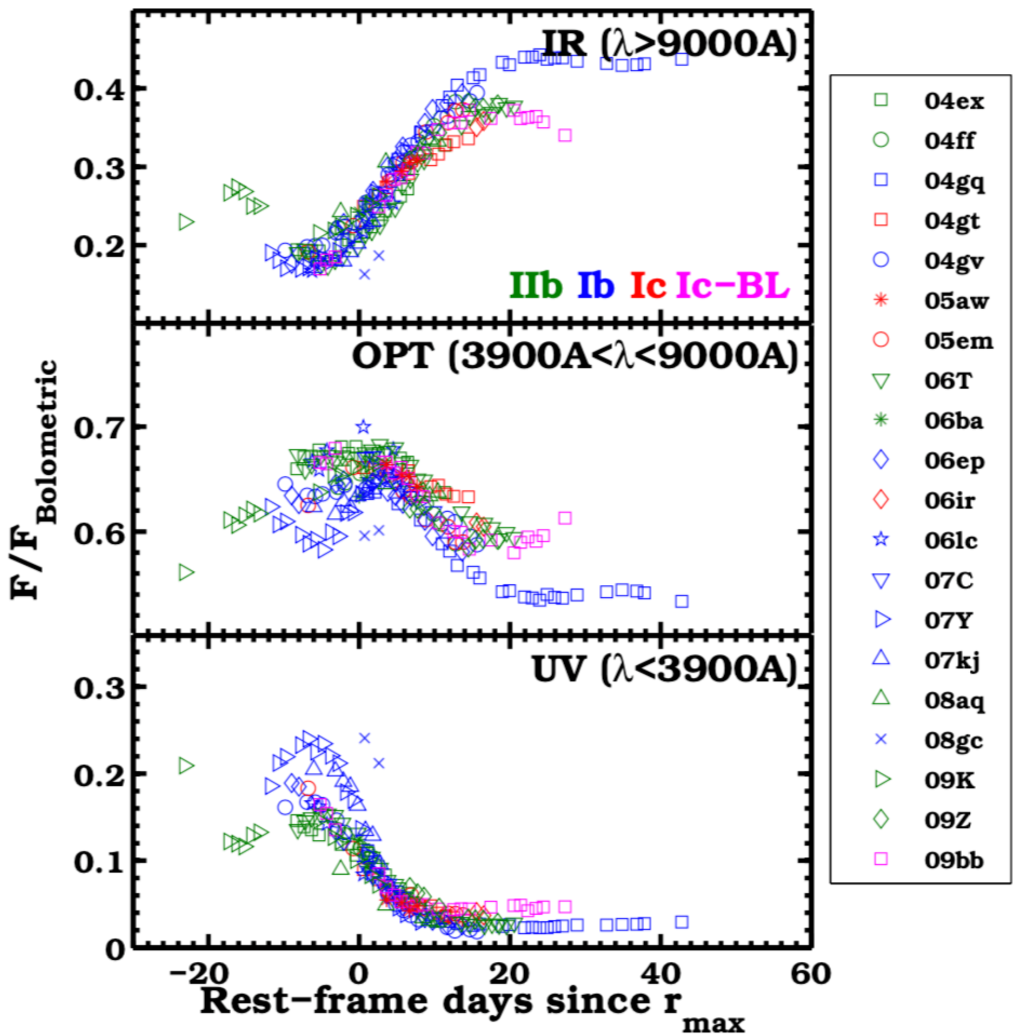

Taddia et al. (2018)

Stripped-envelope SN ejecta properties

- ejecta properties

$$t_{\mathrm{rise}} \propto \kappa^{0.5} M_{\mathrm{ej}}^{3/4} E_{\mathrm{ej}}^{-1/4}$$

$$v_{\mathrm{ej}} \propto E_{\mathrm{ej}}^{1/2} M_{\mathrm{ej}}^{-1/2}$$

- ^{56}Ni mass
  - light curve evolution
    - peak luminosity
    - tail luminosity

Taddia et al. (2018)

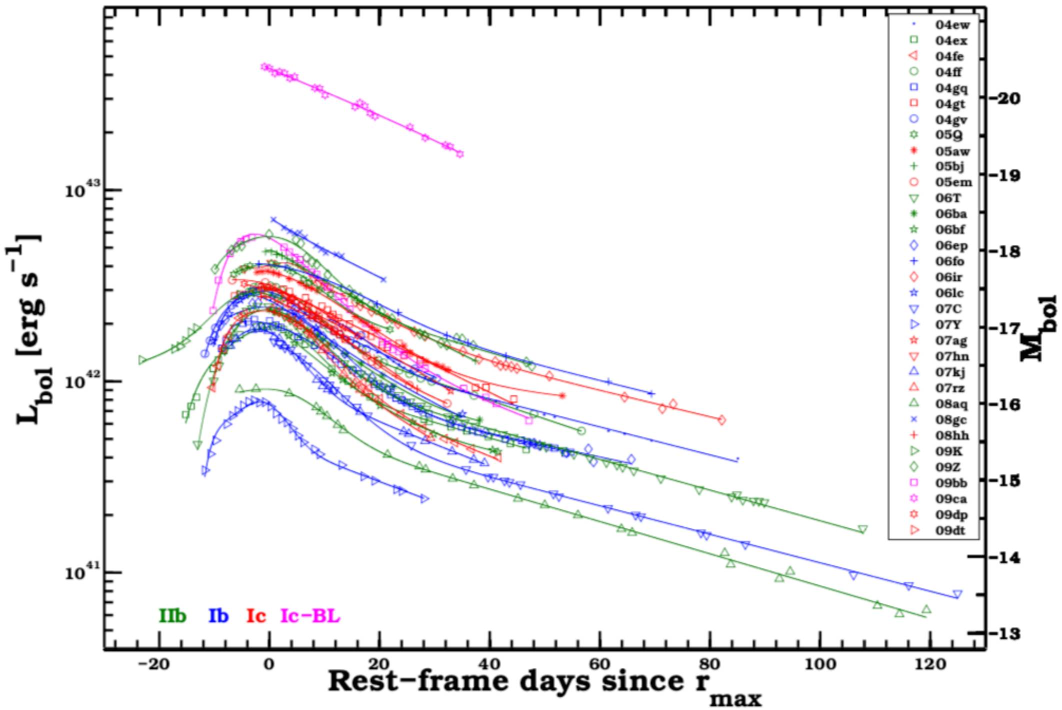

Explosion properties of stripped-envelope SNe

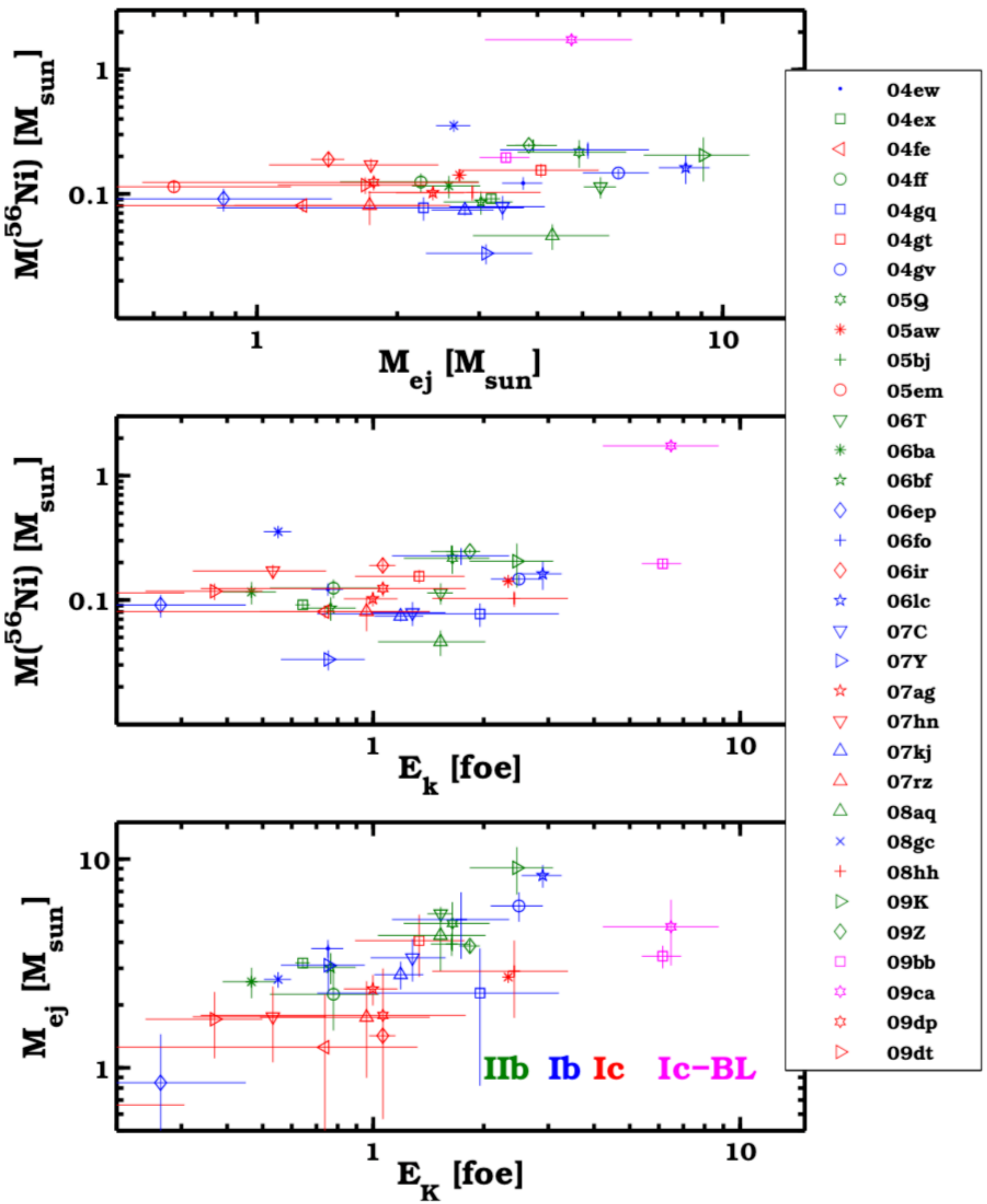

Taddia et al. (2018)

^{56}Ni mass estimates from core-collapse SNe

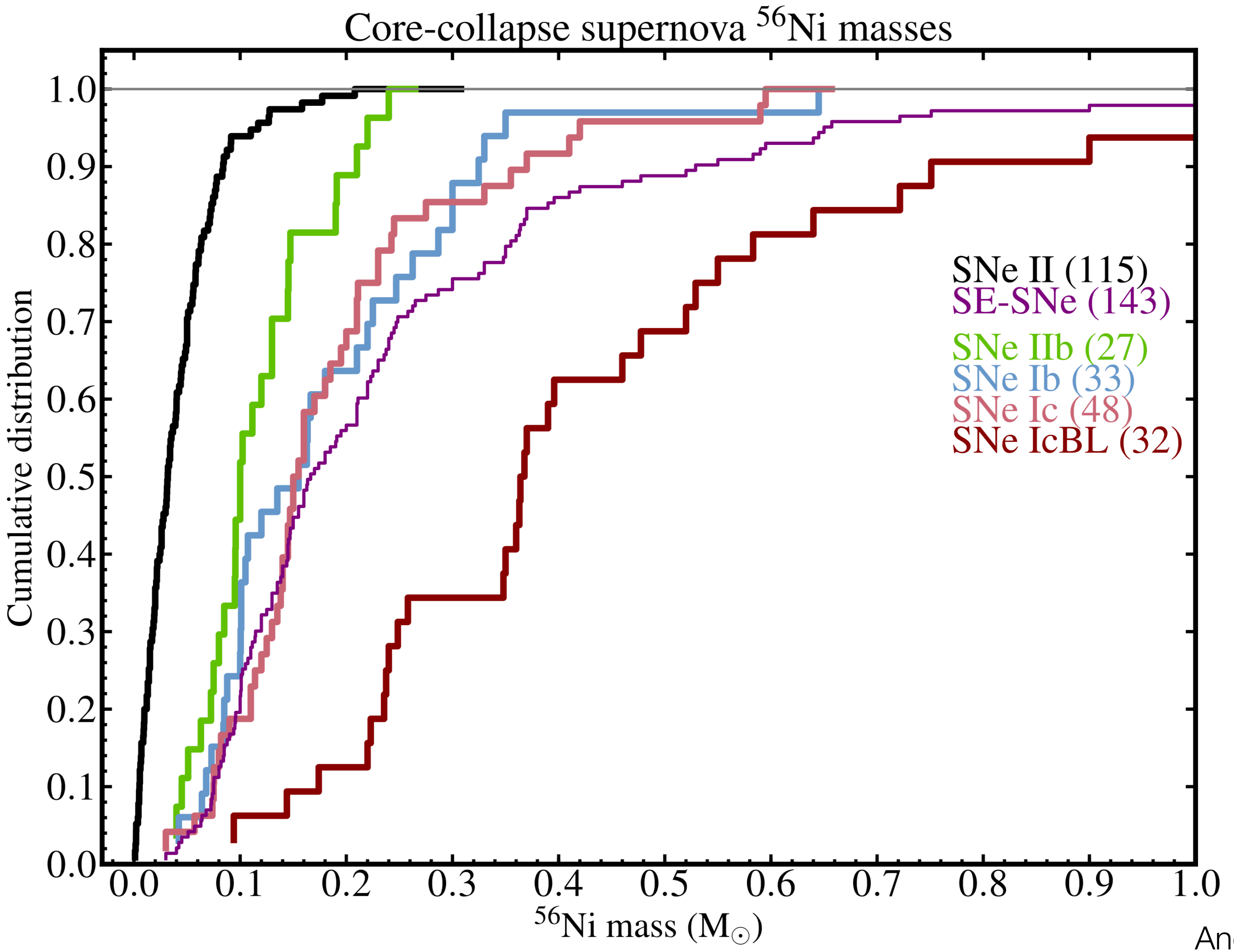

Anderson (2019)

^{56}Ni mass estimates from core-collapse SNe

SN distribution (N)	Mean ($M_\odot$)	Standard deviation ($M_\odot$)	Median ($M_\odot$)	Max ($M_\odot$)	Min ($M_\odot$)
SN II (115)	0.044	0.044	0.032	0.360	0.001
SE-SN (143)	0.293	0.295	0.184	2.400	0.030
SN IIb (27)	0.124	0.061	0.102	0.280	0.030
SN Ib (33)	0.199	0.146	0.163	0.920	0.030
SN Ic (48)	0.198	0.139	0.155	0.840	0.030
SN IcBL (32)	0.507	0.410	0.369	2.400	0.070

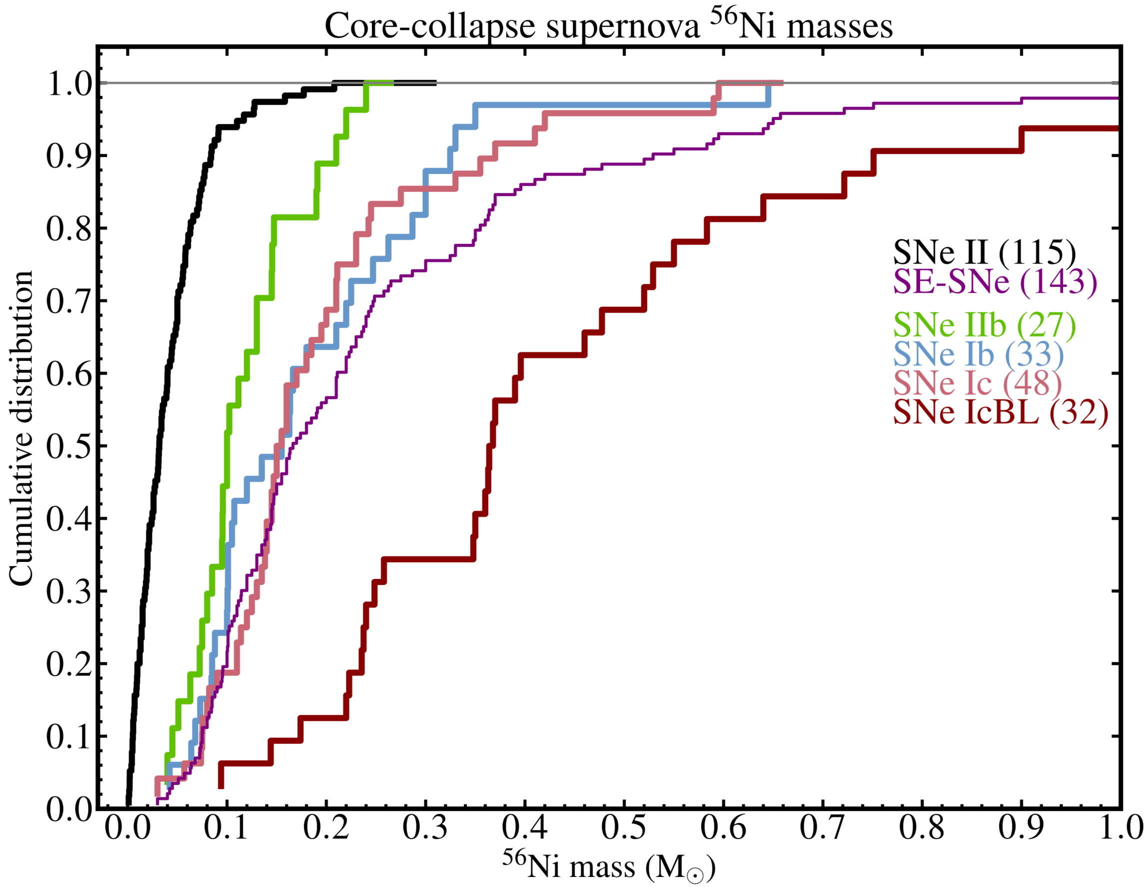

Anderson (2019)

Ejecta mass of stripped-envelope SNe

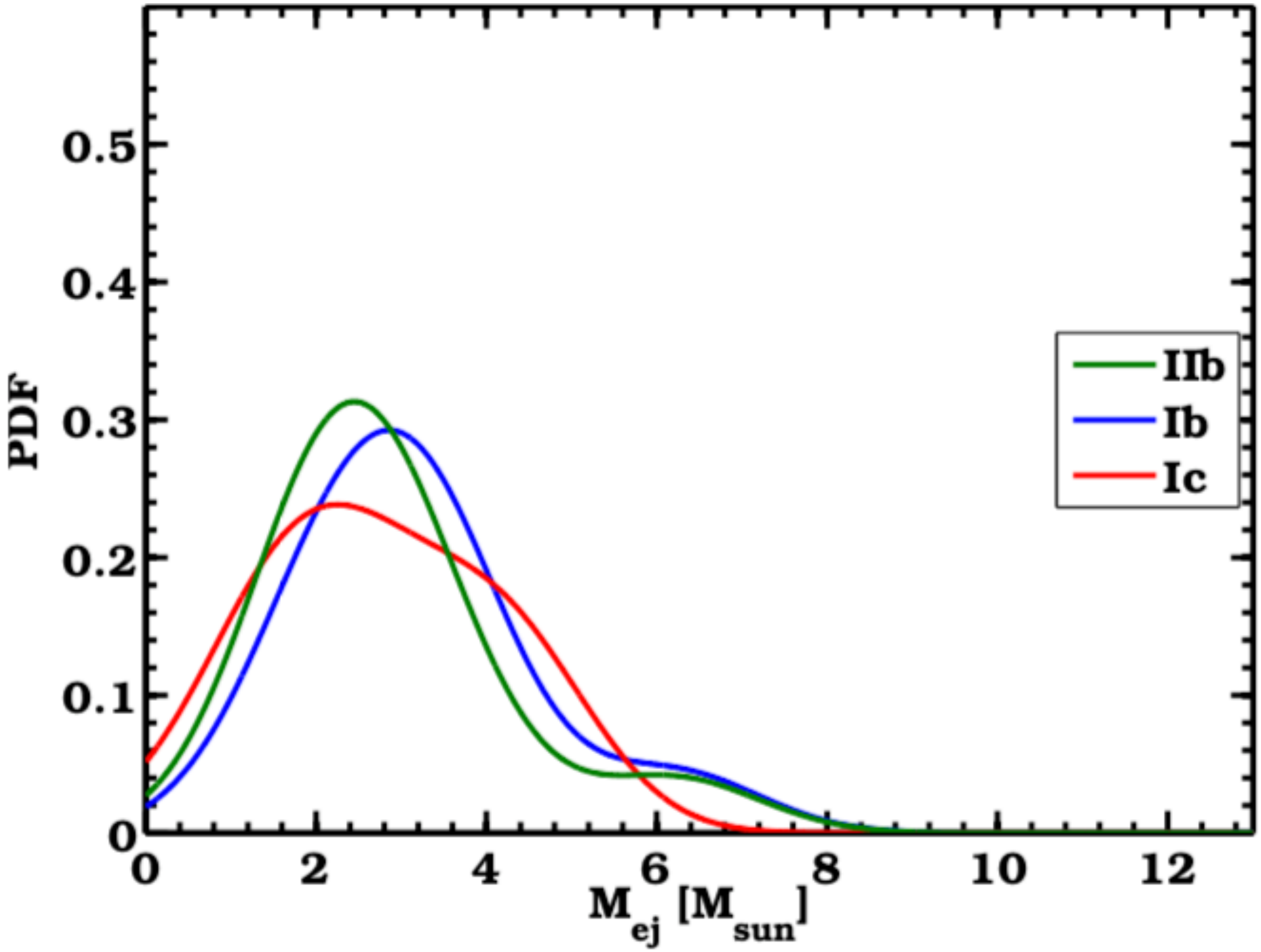

Taddia et al. (2018)

Why is ^{56}Ni mass different?

- initial progenitor mass range and core mass are similar in hydrogen-rich SNe and stripped-envelope SNe

- difference related to binary evolution?

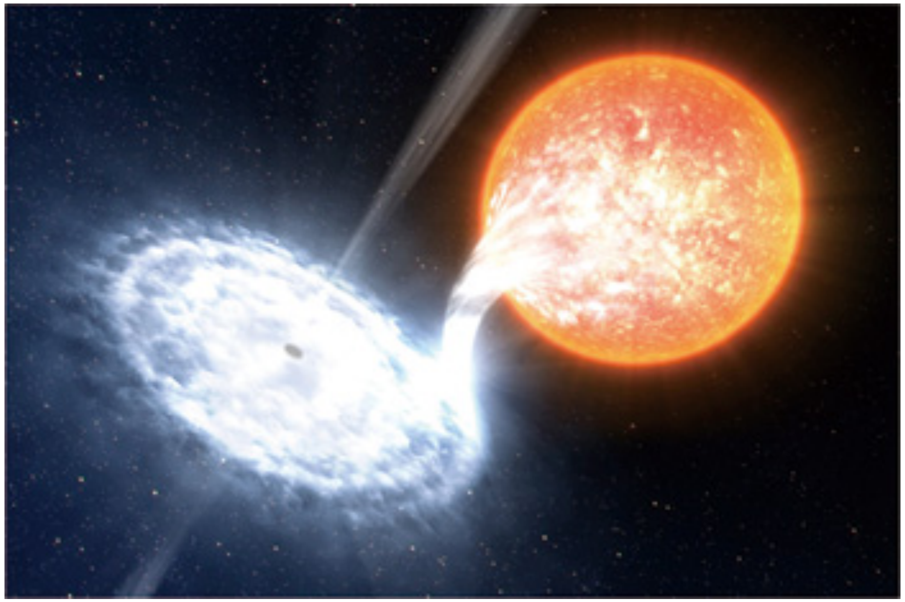

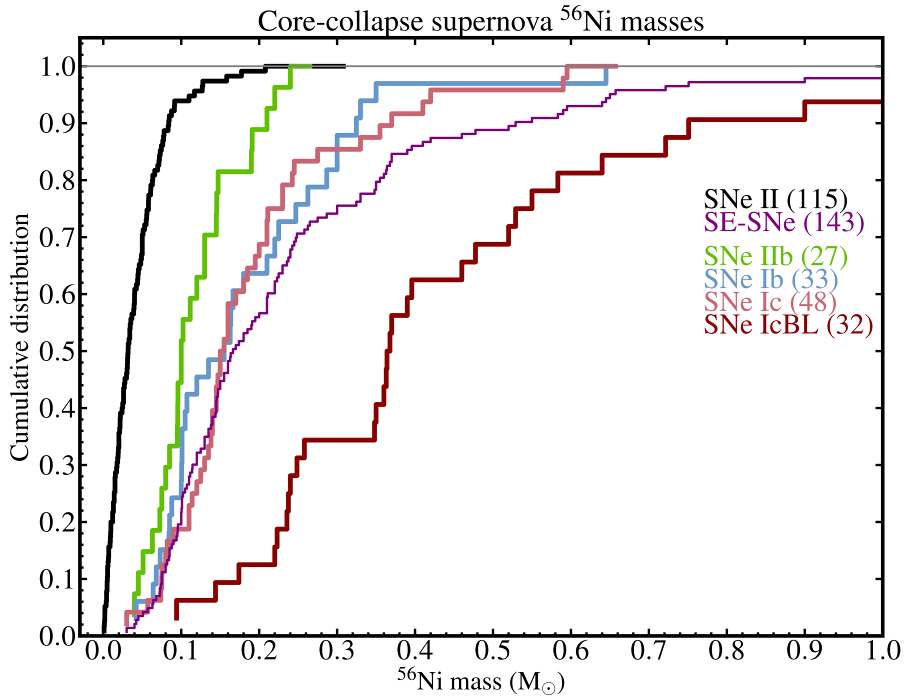

Anderson (2019)

Radio & X-ray to constrain the outermost layers

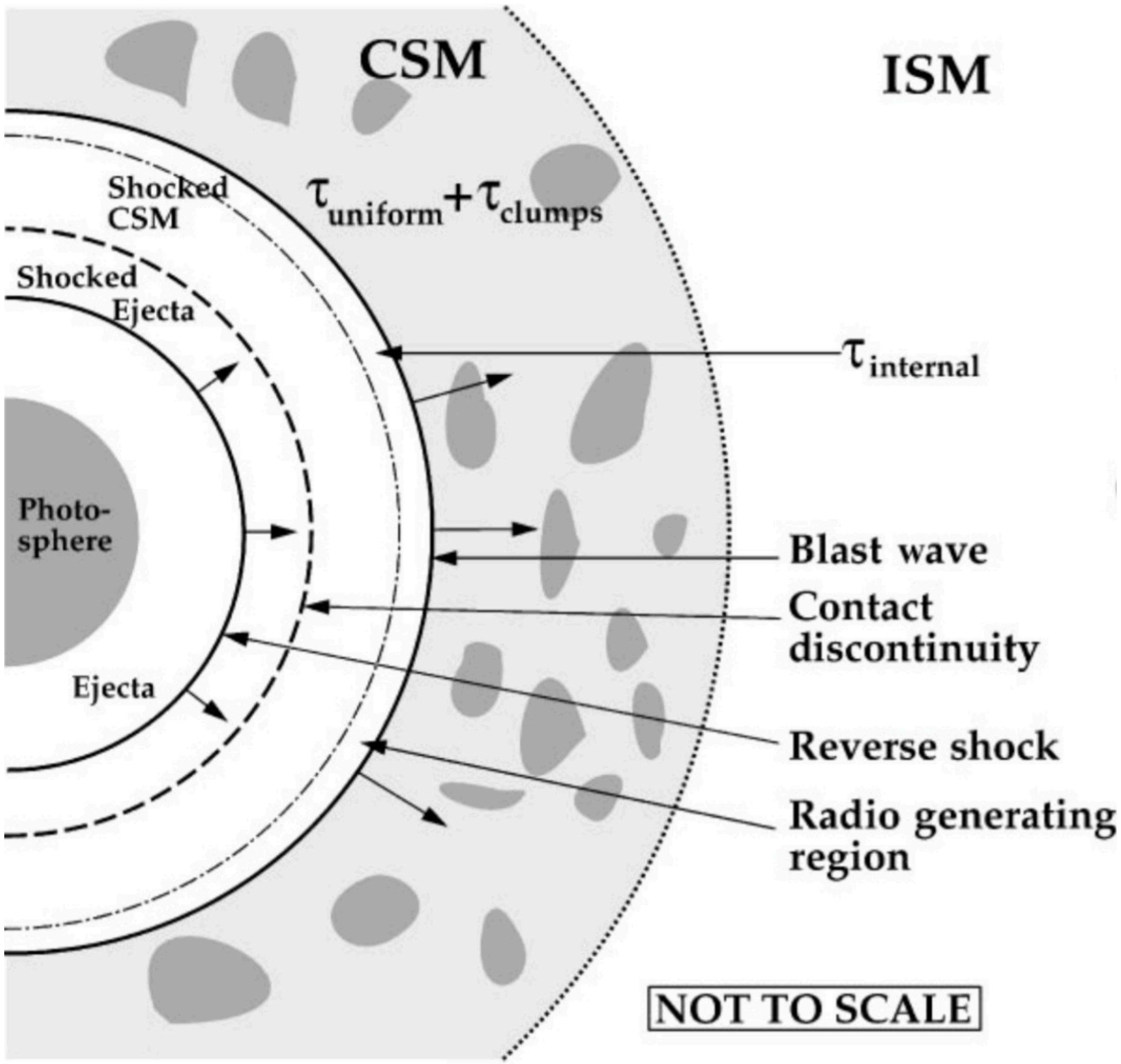

Weiler et al. (2002)

Radio & X-ray to constrain the outermost layers

- intrinsic difference between SNe Ic-BL w/ and w/o a GRB?

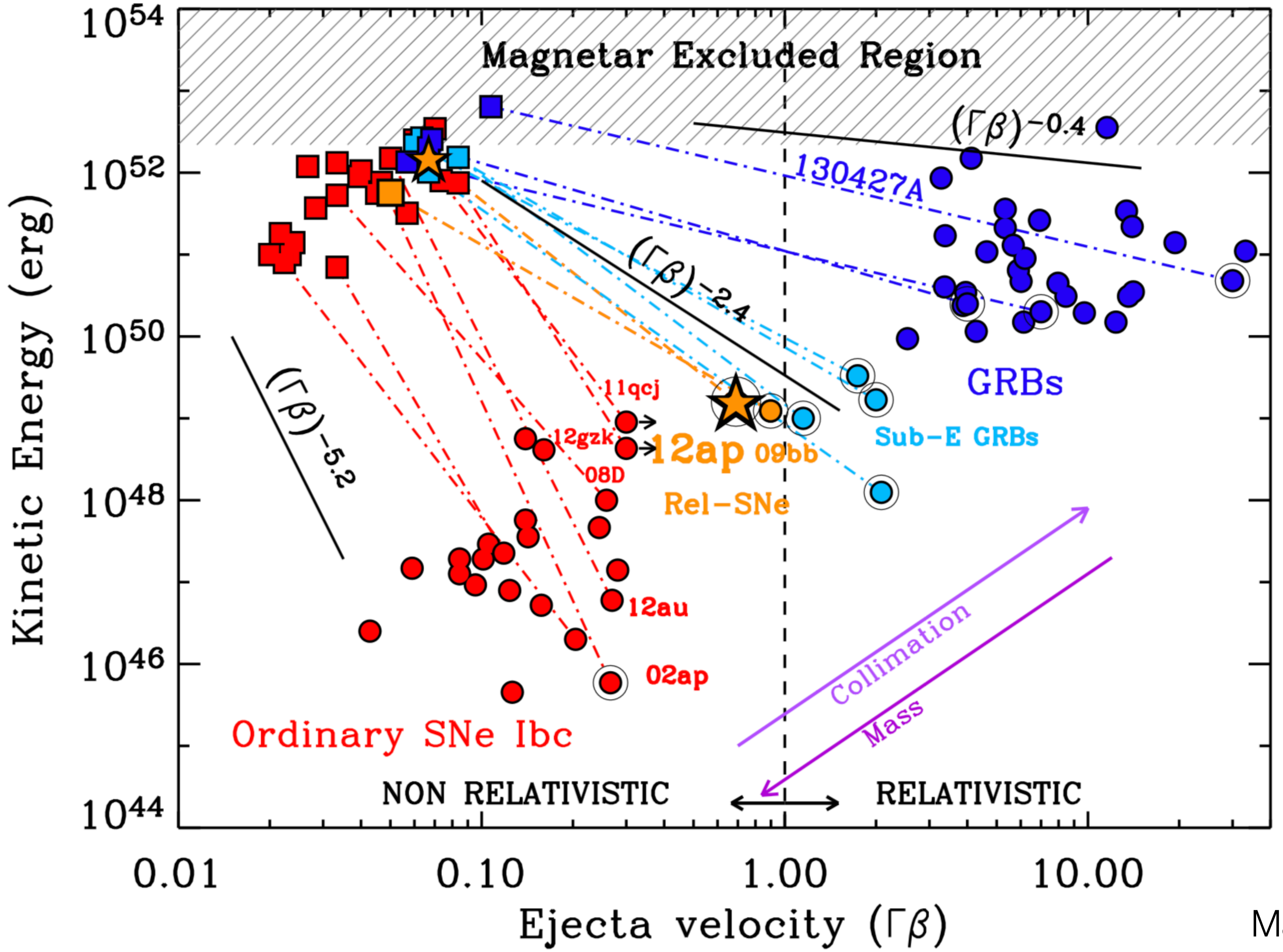

Margutti et al. (2014)

Superluminous SNe

- more than ~ 10 times brighter than other core-collapse SNe
  - often emit more than 10^{51} erg just by radiation

Pastorello et al. (2010)

superluminous supernovae

SNe associated with long GRB

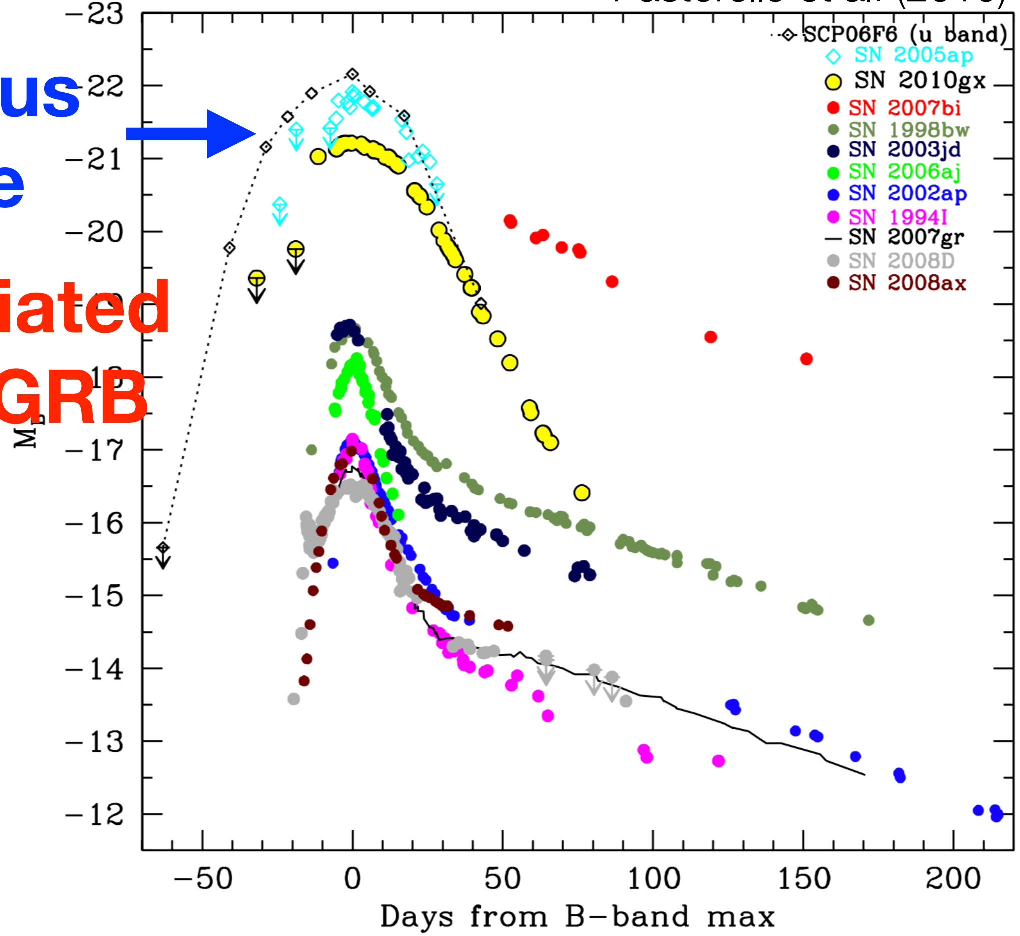

Late-phase spectra: similar to SNe with GRBs

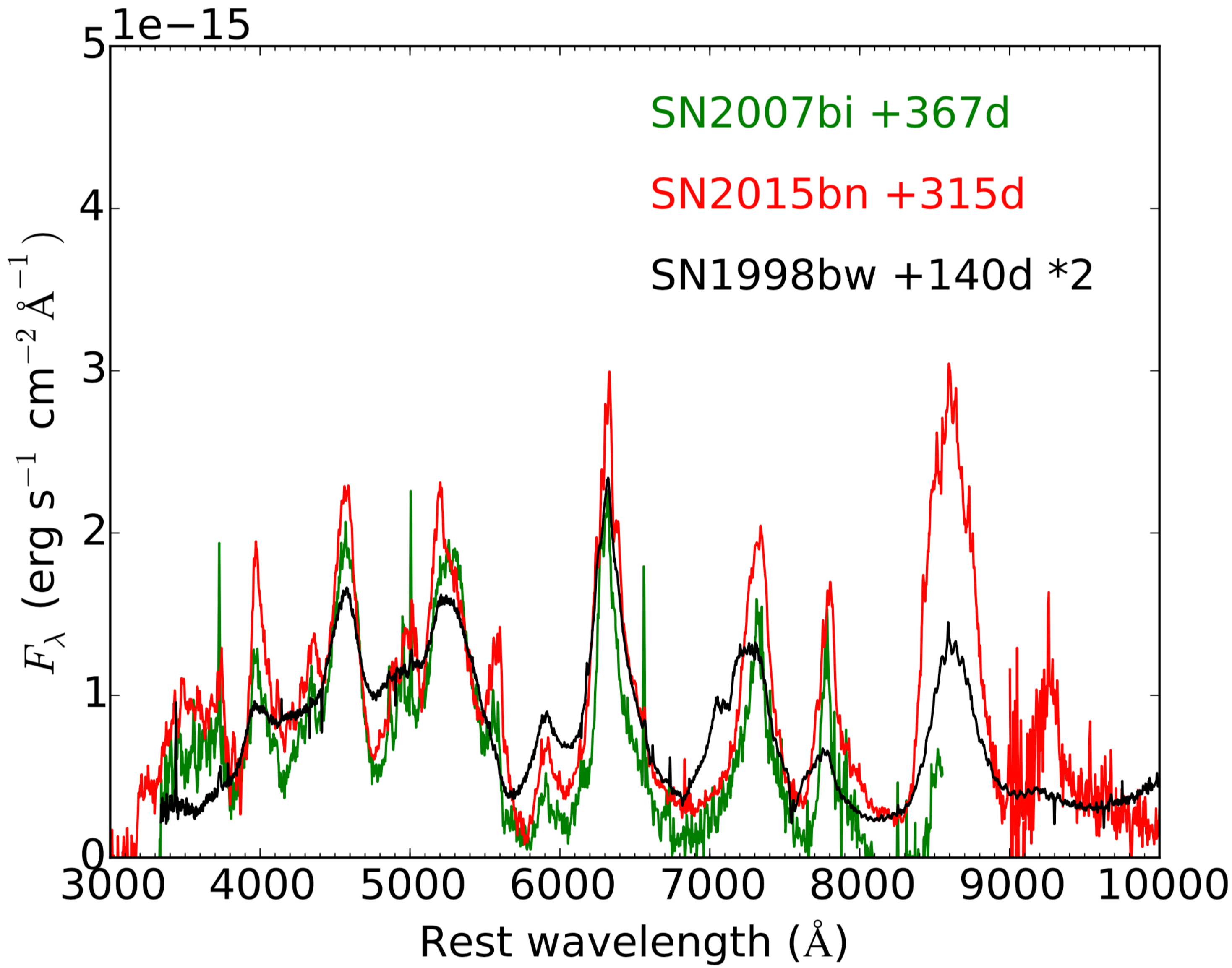

Jerkstrand et al. (2017)

How do they become superluminous?

- large production of ^{56}Ni for SLSNe?
  - more than 5 Msun of ^{56}Ni required
  - light curve decline is often consistent with the ^{56}Co decay
  - rapidly declining SLSNe are inconsistent — another model required

Nicholl et al. (2016)

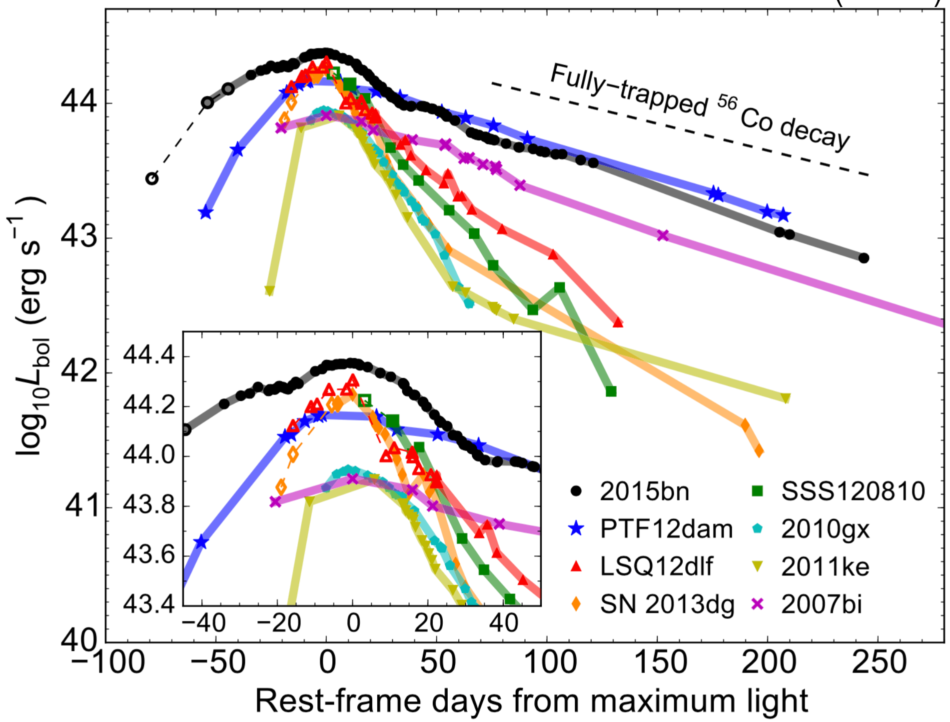

Measuring the ^{56}Ni mass through NIR

- a (PISN) model with large ^{56}Ni mass
  - unblended Fe lines at NIR

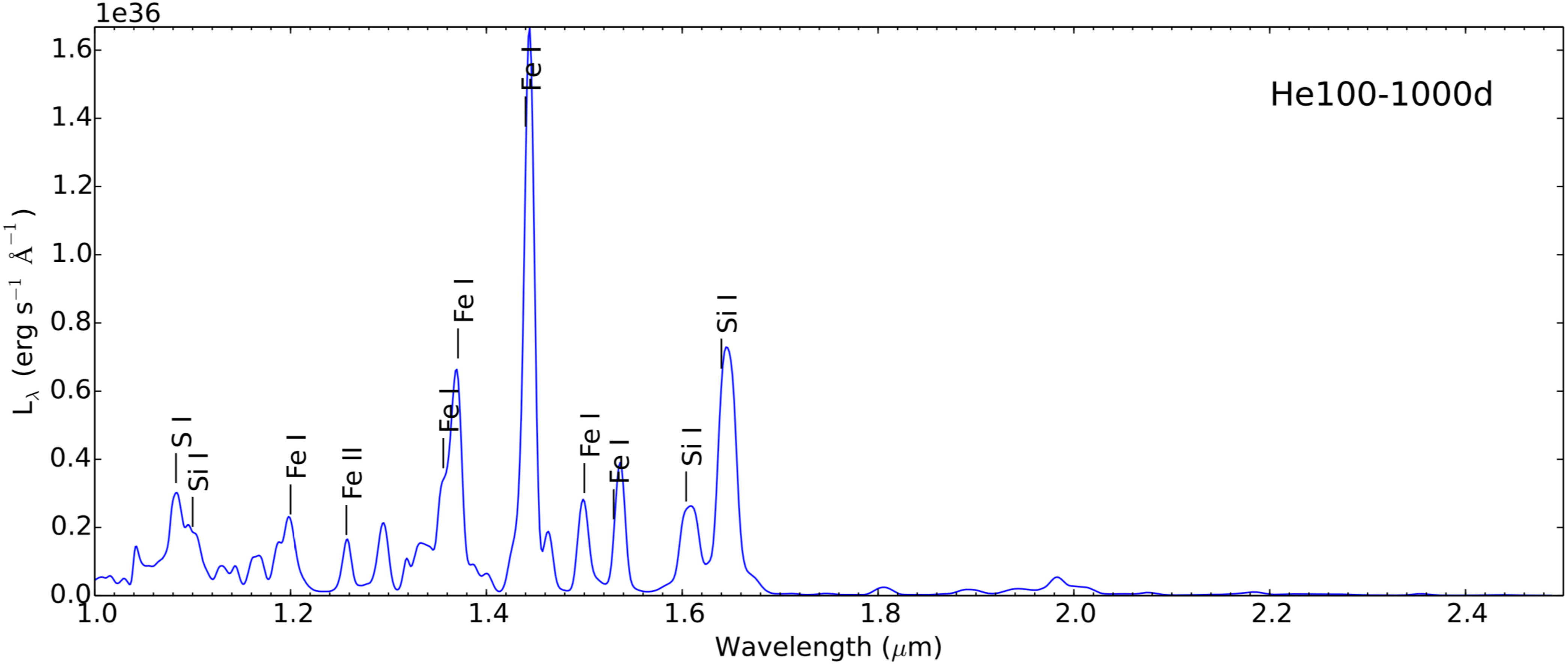

Jerkstrand et al. (2016)

Magnetars

- efficient release of rotational energy of neutron stars (NSs)
  - rotational energy

$$E_{\rm rot} = \frac{1}{2} I_{\rm NS} \Omega^2 \simeq 2 \times 10^{52} \left(\frac{P}{1 \ {\rm ms}} \right)^{-2} {\rm erg}$$

    - SLSNe emit ~ 1e51 erg -> a few ms

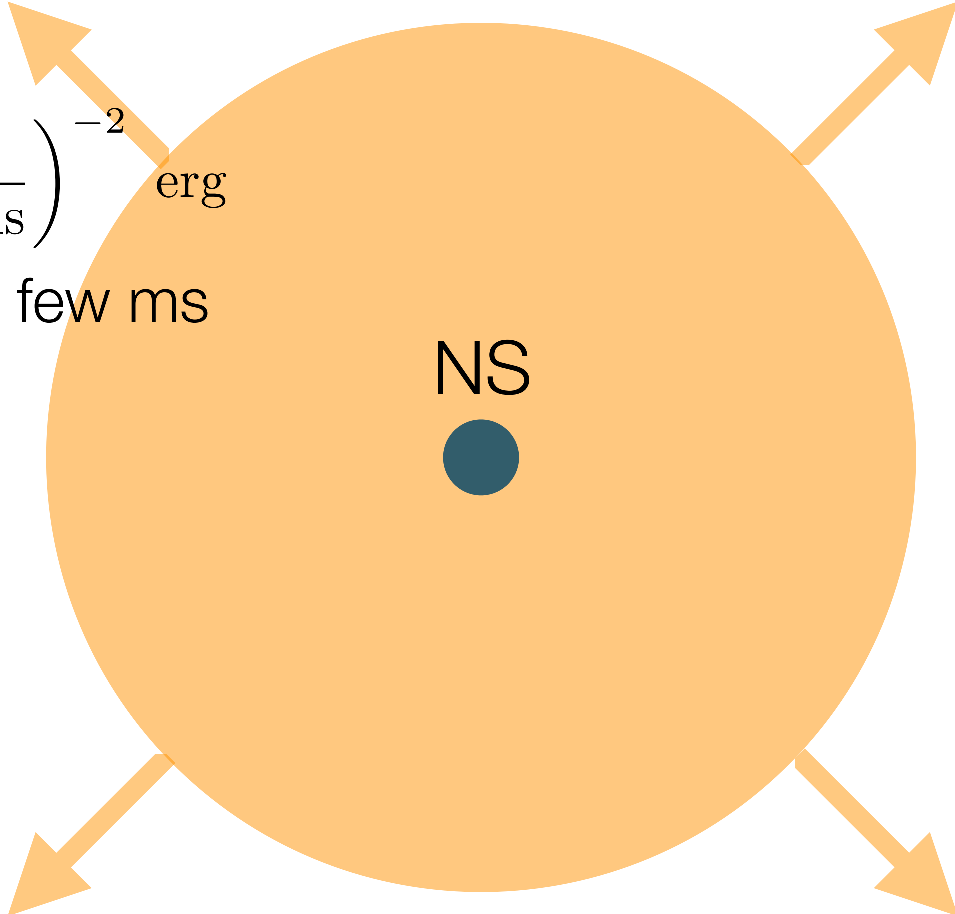

Magnetars

- efficient release of rotational energy of neutron stars (NSs)
  - rotational energy

$$E_{\rm rot} = \frac{1}{2} I_{\rm NS} \Omega^2 \simeq 2 \times 10^{52} \left(\frac{P}{1 \ {\rm ms}} \right)^{-2} {\rm erg}$$

    - SLSNe emit ~ 1e51 erg -> a few ms
  - magnetic field
    - spin down caused by poloidal fields

$$t_m = \frac{6 I_{\rm NS} c^3}{B_{\rm dipole}^2 R_{\rm NS}^6 \Omega^2} \simeq 5 \left(\frac{B_{\rm dipole}}{10^{14} \ G} \right)^{-2} \left(\frac{P}{1 \ {\rm ms}} \right)^2 \ {\rm days}$$

    - SLSN timescales: ~ 10 - 100 days → ~ 1e14 - 1e13 G

magnetar

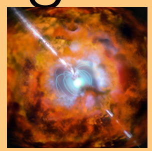

Radio constraints on the magnetar model

- X-ray brightening by “ionization breakout” predicted
  - does not match to observations we have so far

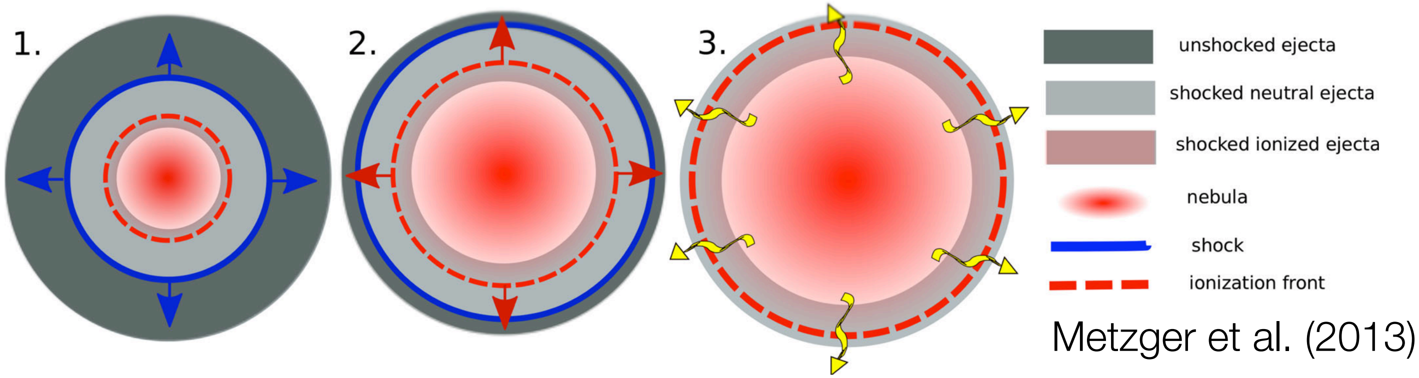

Metzger et al. (2013)

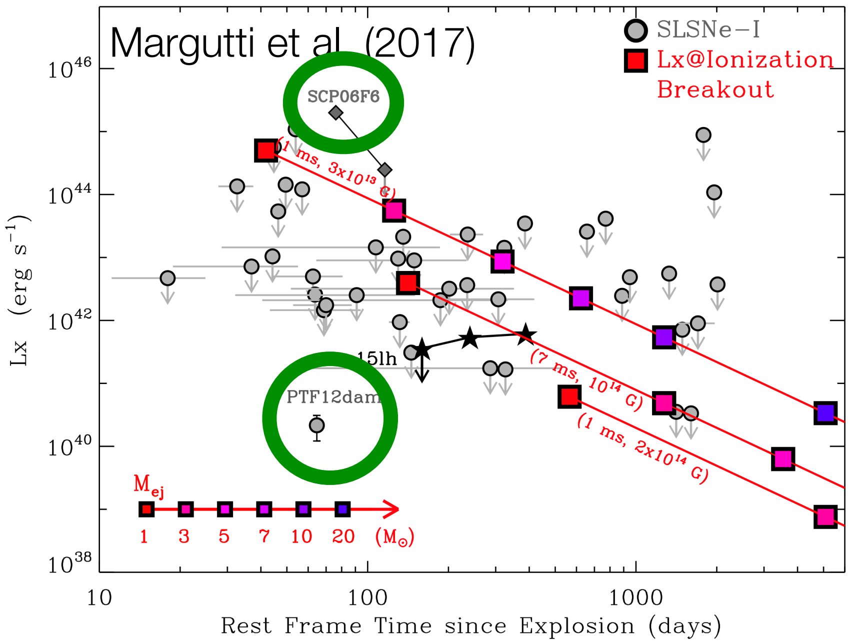

Radio constraints on the magnetar model

- 1 SLSN in 10 SLSNe was detected in radio
    - the origin and association of the radio flux are not clear

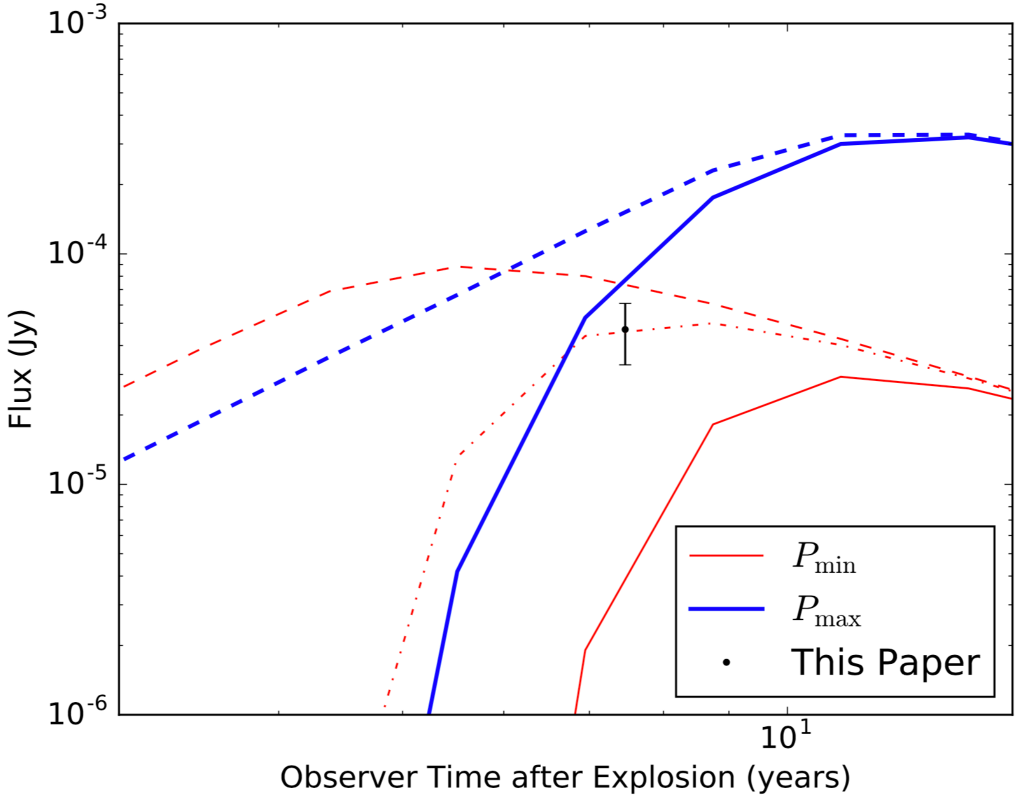

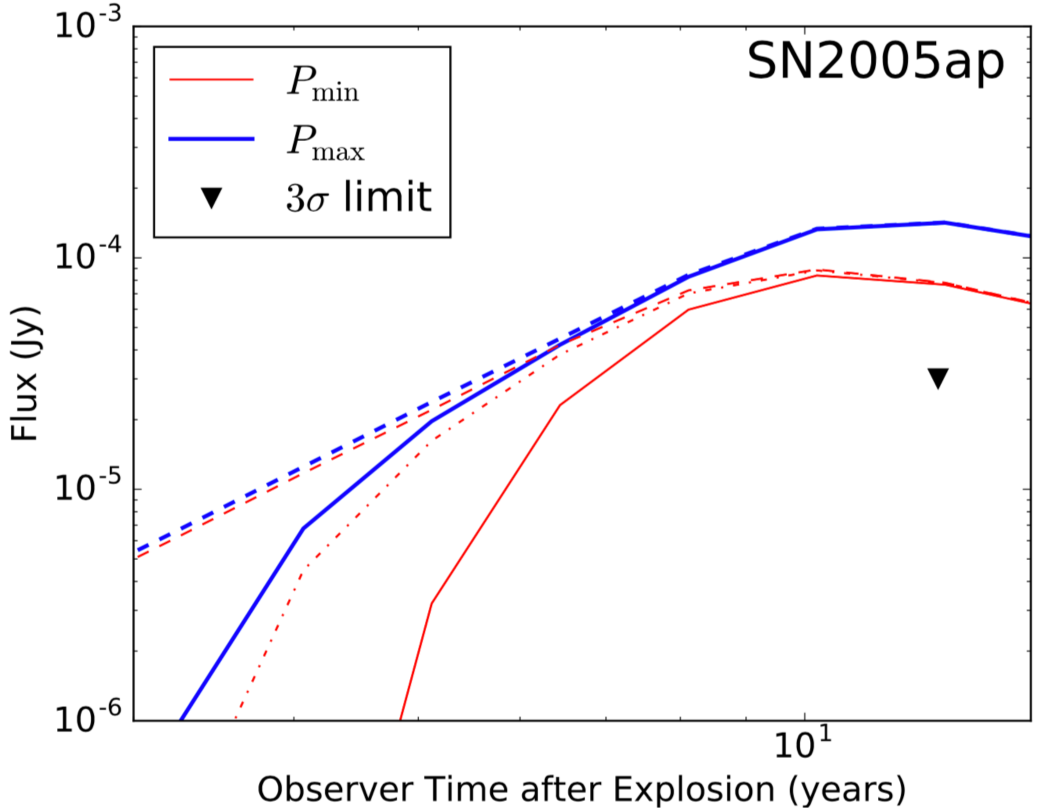

Law et al. (2019)

Summary

- ^{56}Ni mass difference in hydrogen-rich and stripped-envelope SNe
  - they likely come from the same mass range
  - why ^{56}Ni mass has difference?

- X-ray & radio probes outermost layers in SN ejecta
  - SNe Ic-BL w/o GRBs may be intrinsically different from those w/ GRBs

- superluminous SNe
  - the amount of ^{56}Ni needs to be determined by NIR spectra
  - no clear signatures of the proposed central power sources are found in X-rays and radio